

Article

Discovery of a Small-Molecule Modulator of Glycosaminoglycan SulfationSheldon T. Cheung, Michelle S Miller, Reynand Pacoma, Jason
Roland, Jian Liu, Andrew M Schumacher, and Linda C. Hsieh-WilsonACS Chem. Biol., **Just Accepted Manuscript** • DOI: 10.1021/acscchembio.7b00885 • Publication Date (Web): 03 Nov 2017Downloaded from <http://pubs.acs.org> on November 4, 2017**Just Accepted**

“Just Accepted” manuscripts have been peer-reviewed and accepted for publication. They are posted online prior to technical editing, formatting for publication and author proofing. The American Chemical Society provides “Just Accepted” as a free service to the research community to expedite the dissemination of scientific material as soon as possible after acceptance. “Just Accepted” manuscripts appear in full in PDF format accompanied by an HTML abstract. “Just Accepted” manuscripts have been fully peer reviewed, but should not be considered the official version of record. They are accessible to all readers and citable by the Digital Object Identifier (DOI®). “Just Accepted” is an optional service offered to authors. Therefore, the “Just Accepted” Web site may not include all articles that will be published in the journal. After a manuscript is technically edited and formatted, it will be removed from the “Just Accepted” Web site and published as an ASAP article. Note that technical editing may introduce minor changes to the manuscript text and/or graphics which could affect content, and all legal disclaimers and ethical guidelines that apply to the journal pertain. ACS cannot be held responsible for errors or consequences arising from the use of information contained in these “Just Accepted” manuscripts.



Discovery of a Small-Molecule Modulator of Glycosaminoglycan Sulfation

Sheldon T. Cheung,[†] Michelle S. Miller,[†] Reynand Pacoma,[‡] Jason Roland,[‡] Jian Liu,[§] Andrew M. Schumacher,[‡] Linda C. Hsieh-Wilson^{*,†}

[†]Division of Chemistry and Chemical Engineering, California Institute of Technology, 1200 East California Boulevard, Pasadena, California 91125, United States

[‡]Genomics Institute of the Novartis Research Foundation, 10675 John Jay Hopkins Drive, San Diego, California 92121, United States

[§]Division of Chemical Biology and Medicinal Chemistry, Eshelman School of Pharmacy, University of North Carolina, Chapel Hill, North Carolina 27599, United States

ABSTRACT: Glycosaminoglycans (GAGs) play critical roles in diverse processes ranging from viral infection to neuroregeneration. Their regiospecific sulfation patterns, which are generated by sulfotransferases, are key structural determinants that underlie their biological activity. Small-molecule modulators of these sulfotransferases could serve as powerful tools for understanding the physiological functions of GAGs, as well as potential therapeutic leads for human diseases. Here, we report the development of the first cell-permeable, small-molecule inhibitor selective for GAG sulfotransferases, which was obtained using a high-throughput screen targeted against Chst15, the sulfotransferase responsible for biosynthesis of chondroitin sulfate-E (CS-E). We demonstrate that the molecule specifically inhibits GAG sulfotransferases *in vitro*, decreases CS-E and overall sulfation levels on cell-surface and secreted chondroitin sulfate proteoglycans (CSPGs), and reverses CSPG-mediated inhibition of axonal growth. These studies pave the way toward a new set of pharmacological tools for interrogating GAG sulfation-dependent processes and may represent a novel therapeutic approach for neuroregeneration.

INTRODUCTION

Glycosaminoglycans (GAGs) play important roles in a myriad of cellular processes, including viral invasion,¹⁻⁴ cancer metastasis,^{1,5-7} development,^{1,3,8,9} and spinal cord injury.^{7,9-12} Their diverse biological activities are believed to stem from their complex structures, which allow them to interact with a wide range of proteins.^{1,3,7,13,14} GAGs are long, linear polysaccharides that display various patterns of sulfation. For example, chondroitin sulfate (CS) GAGs are assembled from glucuronic acid (GlcA) and *N*-acetylgalactosamine (GalNAc) disaccharide units that contain at least four distinct sulfation motifs: CS-A, CS-C, CS-D, and CS-E.^{7,12} Numerous studies suggest that specific sulfation motifs can serve as key structural elements for protein recognition and the regulation of downstream signaling.^{1,7,14-17}

The sulfation patterns of GAGs are controlled by a family of sulfotransferases.¹⁸⁻²¹ Two major classes of the enzymes, the cytosolic and membrane-associated sulfotransferases, catalyze the transfer of a sulfuryl group from the donor 3'-phosphoadenosine-5'-phosphosulfate (PAPS) to a variety of amine- and hydroxyl-containing substrates.^{18,21} The cytosolic sulfotransferases act on small-molecule substrates such as xenobiotics. With only one exception, the sulfotransferases responsible for modifying GAG polysaccharides are type II transmembrane proteins that reside in the Golgi apparatus. All sulfotransferases have a structurally conserved PAPS-binding site, but distinct acceptor binding sites.^{18,21} Although numerous cytosolic sulfotransferases have been crystallized, only limited structural and functional information on GAG sulfotrans-

ferases is available, which has hindered efforts to design tools to target these enzymes. Indeed, there are no cell-permeable, small-molecule inhibitors of any GAG sulfotransferases. Prior work has focused on peptide- or carbohydrate-based inhibitors²²⁻²⁴ such as sulfated or iminosugars that displayed limited cell permeability due to the presence of charged groups.^{22,23} Thus, despite long-standing interest in inhibiting GAG sulfotransferases,^{25,26} it was unclear whether small molecules could be developed to selectively target this important class of enzymes in a cellular context.

GAG sulfotransferase inhibitors would provide valuable tools for manipulating GAG sulfation patterns and for understanding their roles in biology and disease. The induced expression of specific sulfation motifs is associated with human diseases, including certain cancers,^{27,28} Alzheimer's disease,²⁹ osteoarthritis,^{30,31} malaria,^{32,33} herpes,² and macular corneal dystrophy,³⁴ but surprisingly, pharmacological tools for manipulating GAG sulfation have been lacking. Cellular sulfation levels can be modulated genetically or by using sodium chlorate, which inhibits PAPS synthetase.^{19,20,35-37} However, genetic approaches lack the ease and reversibility of small-molecule inhibitors. Sodium chlorate requires millimolar concentrations and globally affects all sulfotransferases, disrupting the sulfation of hormones, bioamines, xenobiotics, proteins, and other glycans, and inducing off-target effects such as suppression of cell proliferation and replication.³⁵⁻³⁸ Moreover, the toxicity of sodium chlorate due to oxidation of hemoglobin and other metalloproteins limits its biological applications and therapeutic potential.³⁹

Here, we sought to develop selective inhibitors for GAG

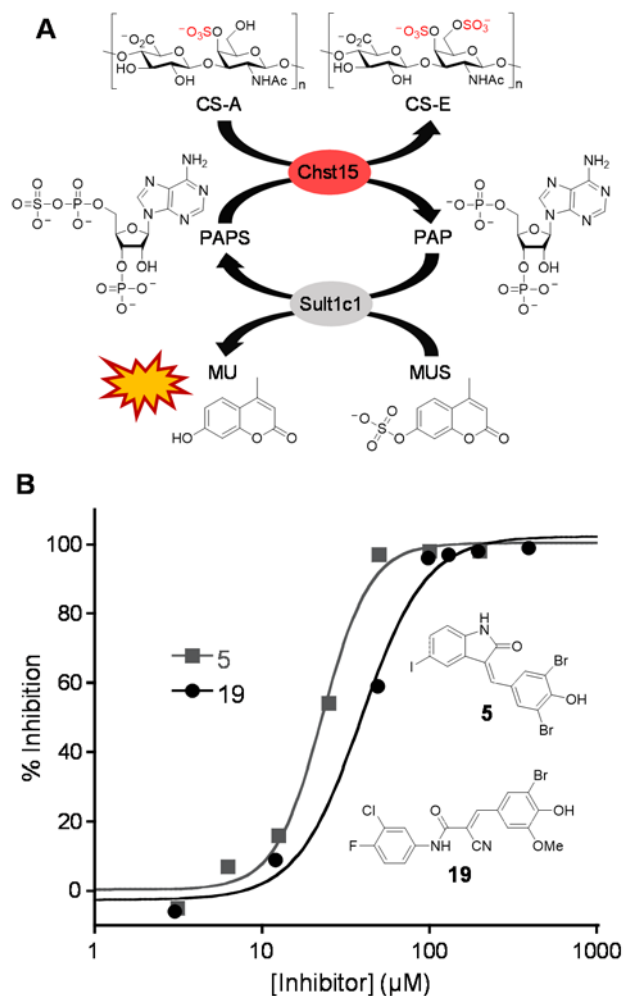


Figure 1. Identification of two lead inhibitor scaffolds. (A) Enzyme-coupled fluorescence assay for the high-throughput screening of small-molecule inhibitors of Chst15. Chst15 activity was monitored by coupling to Sult1c1, which converted MUS to fluorescent MU. (B) Dose-dependent inhibition of Chst15 by compounds **5** and **19** using a [³⁵S]-labeling assay.

sulfotransferases. As a starting point, we targeted Chst15, the chondroitin sulfotransferase responsible for sulfating the 6-*O*-position of *N*-acetylgalactosamine in CS-A to generate CS-E (Figure 1A).^{19,20,40} Previously our laboratory identified the CS-E motif as an important structural determinant in chondroitin sulfate proteoglycans (CSPGs) that inhibits axon regeneration after central nervous system (CNS) injury.¹⁷ Blocking the CS-E motif using a monoclonal antibody specific for CS-E promoted optic nerve regeneration *in vivo*.¹⁷ As such, Chst15 may represent a novel target for neuronal repair after spinal cord injury, stroke, or other injuries.

In this report, we describe the first cell-permeable, small-molecule inhibitors of Chst15 and other GAG sulfotransferases. Using a fluorescence-based, high-throughput screen (HTS), we identified two promising scaffolds that upon structure-activity relationship (SAR) optimization led to molecules with improved potency in biochemical and cellular assays. Kinetic analyses revealed a reversible-covalent mechanism of inhibition, along with good selectivity toward GAG sulfotransferases compared to cytosolic sulfotransferases. Notably, the most potent inhibitor decreased CS-E sulfation levels on CSPGs and reversed the inhibitory activity of CSPGs on axonal growth. These studies open the door to a new set

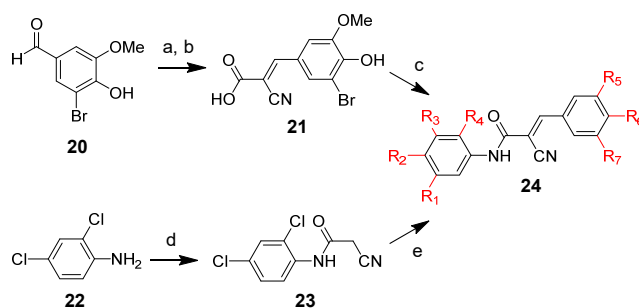
of chemical genetic tools for manipulating and understanding GAG-mediated events, as well as a novel potential therapeutic strategy for neuroregeneration.

RESULTS AND DISCUSSION

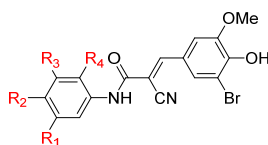
To discover molecules that inhibit Chst15, we developed a fluorescence-based assay in which Chst15 activity was coupled to the enzyme Sult1c1 (Figure 1A). Sult1c1 converts 3'-phosphoadenosine-5'-phosphate (PAP) to PAPS by using 4-methylumbelliferyl sulfate (MUS) as the sulfate donor, resulting in liberation of fluorescent 4-methylumbelliferone (MU).^{41,42} We optimized and validated the assay in 96-well plates to obtain a Z-factor value suitable for high-throughput screening (0.62; Figure S1). The assay was then miniaturized to a 1536-well plate format, and a diversity set of 70,000 compounds was screened at 12.5 μM for its ability to inhibit human Chst15. The hits obtained were counter-screened against Sult1c1, resulting in nineteen compounds (renumbered **1-19**) that inhibited Chst15 with little or no Sult1c1 inhibition (Figure S2A). To validate these compounds further, we used a direct, sensitive assay that monitored [³⁵S]-incorporation from [³⁵S]-PAPS into CS-A (Figure S2B). The top compounds, **5** and **19**, exhibited significant dose-dependent inhibition of Chst15 with IC₅₀ values of 23 μM and 39 μM, respectively (Figure 1B).

To further evaluate **5**, we re-tested its activity and that of several commercially available analogs using the [³⁵S]-labeling assay (Figure S3). Although **5** effectively inhibited Chst15, none of the analogs showed improved inhibition, and **5** also unexpectedly showed cross-reactivity toward Sult1c1 when re-evaluated in the counter-screen (12.5 μM, Figure S4). We therefore focused our attention on **19**. Thirty-one analogs of **19** were synthesized or obtained commercially (Tables 1 and 2; Figure S5). To facilitate diversification of the molecule, we devised two synthetic routes that allowed for modification of the anilide or vinylbenzene moieties (Scheme 1). Initial formation of the α,β-unsaturated acid followed by an *N,N*-diisopropylcarbodiimide (DIC)-promoted amide bond coupling enabled functional groups around the anilide to be altered. Alternatively, synthesis of the cyanoacetamide in two steps permitted incorporation of different vinylbenzene substituents by a piperidinium acetate-catalyzed Knoevenagel condensation. These routes enabled the installation of a wide range of functionalities from a

Scheme 1. Synthesis of Analogs of **19**^a

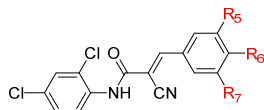


^aReagents and conditions: (a) ethyl cyanoacetate, piperidine, AcOH, PhMe (91%); (b) NaOH, THF (77%); (c) Ar-NH₂, DIC, THF (17-56%); (d) cyanoacetic acid, DIC, THF (45%); (e) Ar-CHO, piperidine, AcOH, PhMe (52-93%). See Table 1, Table 2, and Figure S5 for specific structures.

Table 1. Relative Inhibition of Chst15 by Anilide Analogs^a

Compound	R ₁	R ₂	R ₃	R ₄	Relative Inhibition
19	H	F	Cl	H	1.00 ± 0.01
25	H	F	H	H	0.19 ± 0.00
26	H	Cl	H	H	0.30 ± 0.04
27	H	Br	H	H	0.10 ± 0.00
28	H	Me	H	H	0.08 ± 0.00
29	H	CF ₃	H	H	0.10 ± 0.00
30	H	tBu	H	H	0.35 ± 0.05
31	H	H	H	Cl	0.57 ± 0.02
32	H	H	H	F	0.37 ± 0.00
33	H	H	Ph	H	0.07 ± 0.01
34	H	Cl	H	Cl	1.35 ± 0.12
35	Cl	H	Cl	H	0.98 ± 0.10
36	Cl	H	H	Cl	1.21 ± 0.09

^aRelative inhibition values were determined from three independent measurements using 25 μM of inhibitor and normalized to the inhibition by compound **19**.

Table 2. Relative Inhibition of Chst15 by Vinylbenzene-Analogs^a

Compound	R ₅	R ₆	R ₇	Relative Inhibition
34	OMe	OH	Br	1.35 ± 0.12
37	OMe	OH	H	0.13 ± 0.00
38	OMe	OH	F	0.40 ± 0.03
39	OMe	OH	Cl	0.49 ± 0.01
40	OMe	OH	I	0.88 ± 0.02
41	H	OH	Br	0.32 ± 0.00
42	Br	OH	Br	0.97 ± 0.10
43	OEt	OH	Br	1.26 ± 0.16
44	OMe	H	Br	0.00 ± 0.00
45	OMe	NH ₂	Br	0.32 ± 0.01

^aSee footnote from Table 1.

large pool of commercially available anilines and benzaldehydes.

We compared the inhibitory activities of the analogs using the [³⁵S]-labeling assay. Removal of either aromatic ring on **19** (**21**, **23**, **46**, Scheme 1 and Figure S5) abolished activity, and changing the anilide ring from di- to mono-substitution (**25-33**) greatly reduced its potency (Table 1 and Figure S5). Altering the position of mono-substitution (**31**, **32**) did not change this trend, nor did substitution with larger groups such as *tert*-butyl (**30**), phenyl (**33**), or fused-phenyl substituents (**48**, Figure S5). The importance of di-

substitution was highlighted further upon analysis of various di-chloro-substituted analogs (**34-36**), which had comparable or greater potency than the original compound **19**. In particular, compound **34** showed 35% greater potency when compared to **19** in the [³⁵S]-labeling assay.

We next explored the importance of the vinylbenzene substituents by synthesizing analogs derived from **34**. Removal of any of the three substituents on the vinylbenzene ring (**37**, **41**, **44**) greatly attenuated the inhibitory potency of the compound (Table 2). Replacement of the bromo substituent with other halogens (**38-40**) decreased the activity by up to 2.5-fold, suggesting that the stereoelectronic properties of the bromo group are well suited for binding the enzyme. By comparison, modifications to the methoxy group were more tolerated. For example, replacement of the methoxy with a bromo group (**42**) led to no significant change in potency, while replacement with an ethoxy group (**43**) enhanced potency by 26% as compared to **19**. However, neither of these analogs exhibited improved potency when compared to **34**. Meanwhile, modification of the phenol group to aniline (**45**) or indazole (**49**, Figure S5) decreased the potency by 3-fold and 26-fold, respectively. Methylation of the phenol functionality also drastically lowered the inhibitory potency for compounds with common scaffolds (*e.g.* **35** vs. **47**, Table 1 and Figure S5). Thus, the hydrogen bonding and electronic properties of the phenolic hydroxyl group are important for Chst15 inhibition.

We hypothesized that the α,β-unsaturated cyanoacrylamide moiety might serve as an electrophile for nucleophilic amino acid side chains. Indeed, cyanoacrylamide compounds have been reported to inhibit kinases via a reversible covalent mechanism by reacting with noncatalytic cysteine residues.^{43,44} Rotating frame nuclear Overhauser effect spectroscopy (ROESY) data suggested that the *E*-isomer is generated in **34** after the Knoevenagel condensation (Figure S6). Specifically, correlations between the amide and alkene protons of **34** were detected, which is only possible in the *E*-configuration. Reduction of this *E*-olefin using Pd/C abolished the dose-dependent effects of **34** (**50**, Figure S5).

To investigate the electrophilic potential of **34**, we incubated it with a surrogate nucleophile, β-mercaptoethanol (BME, Figure S7A). Consistent with the formation of a covalent thioether adduct,⁴³ we observed a decrease in the UV-visible absorption band corresponding to the cyanoacrylamide moiety (λ_{max} = 378 nm; Figure S7B). Upon ten-fold dilution of the sample treated with BME into phosphate buffered saline (PBS), the absorbance was restored as compared to dilution into PBS containing BME, suggesting that formation of the adduct was reversible (Figure S7C). Further evidence for a reversible covalent adduct was obtained by ¹H NMR spectroscopy (Figure S7D). Incubation of **34** with BME led to partial loss of the olefinic proton (δ = 7.83 ppm) and appearance of an aliphatic β-proton (δ = 4.49 ppm). Peak integrations indicated that ~57% of the population had formed the thioether adduct, and this population was reduced to ~37% upon two-fold dilution into PBS.

We also examined whether **34** inhibits Chst15 through a reversible covalent mechanism by pre-incubating the inhibitor with Chst15 for various lengths of time. Longer pre-incubation times lead to greater inhibition of the enzyme, consistent with a covalent mechanism of action (Figure S8A). However, unlike the inhibition typically observed with irreversible covalent inhibitors, the activity of Chst15 was rapidly restored in ten-fold dilution experiments

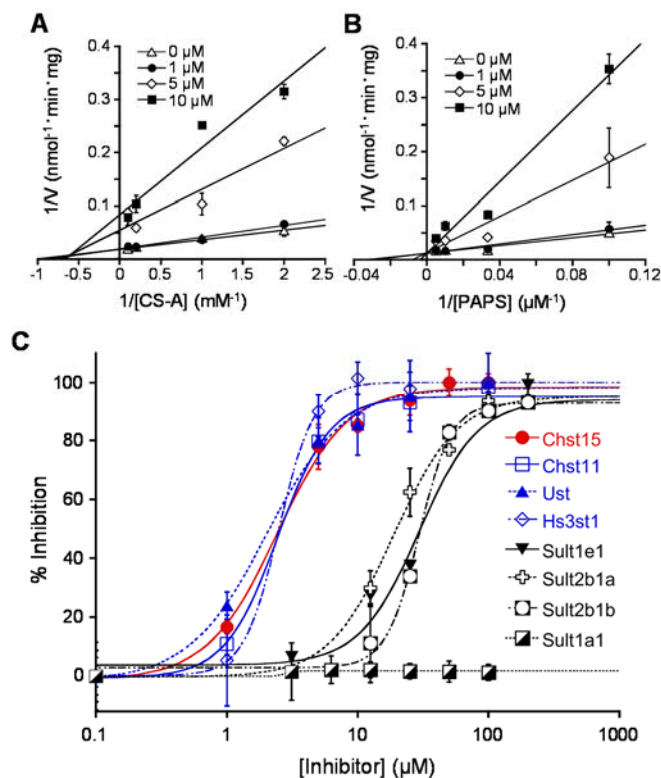


Figure 2. Kinetic analysis and specificity of compound **34**. Pseudo first-order studies using the enzyme-coupled fluorescence assay revealed a competitive and mixed mode of inhibition for the substrates (A) PAPS and (B) CS-A, respectively. (C) Compound **34** displayed 8- to 18-fold greater specificity for GAG sulfotransferases compared to cytosolic sulfotransferases.

even at high concentrations of **34** (up to 100 μM). These observations suggest dissociation of the enzyme-inhibitor complex, thus supporting its reversibility (Figure S8B).

To study the mechanism further, we performed pseudo first-order kinetic analyses with compound **34**. When the CS-A substrate concentration was varied under pseudo first-order conditions with respect to PAPS, we obtained K_i and K' values of 1.43 μM and 2.45 μM , respectively, and observed a shift in both V_{max} and K_m indicative of a mixed mode of inhibition (Figure 2A, Table S1, Figure S10). However, when the PAPS concentration was varied under pseudo first-order conditions with respect to the CS-A acceptor substrate, we observed a competitive mode of inhibition with a K_i value of 0.77 μM (Figure 2B, Table S1, Figure S10). Taken together, these results suggest that inhibitor **34** competitively interacts with the PAPS binding site and also likely engages part of the acceptor binding site.

Due to its electrophilic mechanism of action, **34** could potentially react with numerous proteins that contain reactive cysteine residues. Cravatt and co-workers have previously identified reactive cysteine-containing proteins using the iodoacetamide-alkyne probe **51** (Figure S9A), which alkylates reactive cysteine residues and allows for visualization of the proteins following copper-catalyzed azide-alkyne cycloaddition (CuAAC).⁴⁵ Among the most highly reactive proteins were thioredoxin, protein arginine methyltransferase 1 (PRMT1), aldehyde dehydrogenase 1A (ALDH1A), acetyl-CoA acetyltransferase 1 (ACAT1), and glutathione S-transferase omega 1 (GTSO1). We incubated each of these pro-

teins with iodoacetamide probe **51** (25 μM) in the presence or absence of **34** (10 and 25 μM) for 2 h at room temperature, and then reacted them with 5-carboxytetramethylrhodamine-azide (azido-TAMRA). Importantly, no decrease in the labeling of any of the proteins by **51** was observed, as visualized by in-gel fluorescence (Figure S9B). These data indicate that compound **34** does not react non-specifically with some of the most reactive cysteine residues in the proteome. As further evidence, we incubated Neu7 astrocytes in the presence or absence of **34** (25 μM) for 24 h, followed by treatment with **51** for 1 h. Again, the labeling of proteins by iodoacetamide probe **51** was unchanged upon treatment with **34** (Figure S9B). Together, our studies provide strong evidence that inhibitor **34** is selective for sulfotransferases over the myriad of reactive cysteine-containing proteins in the proteome.

We next investigated the specificity of **34** against a series of cytosolic and GAG sulfotransferases. Importantly, we observed a clear dichotomy in the ability of **34** to inhibit GAG sulfotransferases compared to cytosolic sulfotransferases (Figure 2C). While **34** inhibited Chst15 and other closely related GAG sulfotransferases such as the chondroitin 4-*O*-sulfotransferase Chst11, the chondroitin 2-*O*-sulfotransferase Ust, and the heparan 3-*O*-sulfotransferase Hs3st1 (IC_{50} values 2.0-2.5 μM), its activity against the cytosolic sulfotransferases Sult1e1, Sult2b1a, and Sult2b1b, which modify steroidal substrates, was significantly lower (IC_{50} values 19-42 μM). Moreover, **34** showed no activity against the cytosolic sulfotransferase Sult1c1 used in the enzyme-coupled assay at the concentrations tested (3-100 μM). Inhibition of other GAG sulfotransferases by **34** is consistent with the high sequence homology (25-81%) shared by GAG sulfotransferases^{40,46,47} and our observations that **34** engages the PAPS binding pocket.

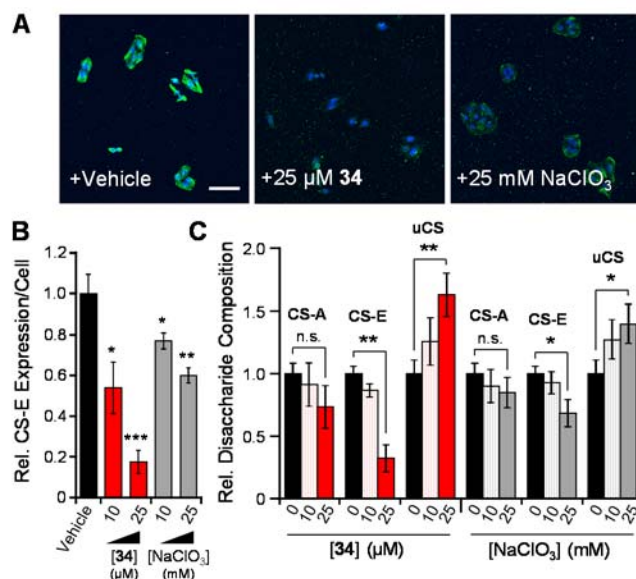


Figure 3. Treatment of Neu7 astrocytes with **34** reduces expression of CS-E on cell-surface and secreted CSPGs. (A) Representative images of Neu7 astrocytes treated with **34** or chlorate and co-stained with a CS-E-specific antibody (green) and the nuclear stain DAPI (blue). (B) Quantification of the average fluorescence from anti-CS-E immunostaining under each condition. Values represent the mean \pm S.E.M. from three experiments. $n = 20$ -100 cells per experiment. (C) CS-A, CS-E, and uCS disaccharide composition of secreted CSPGs from Neu7 astrocytes treated with **34** or sodium chlorate. $n = 3$. * $P < 0.05$, ** $P < 0.01$, *** $P < 0.001$, n.s. = not significant. For B, P values are calculated relative to the vehicle control. (Scale bar: 100 μm .)

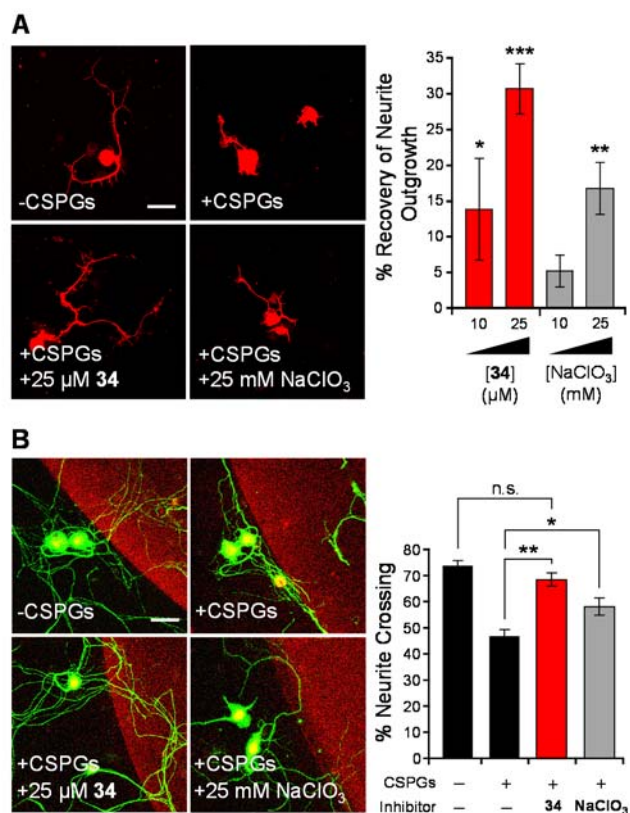


Figure 4. Treatment of Neu7 astrocytes with **34** attenuates CSPG-mediated inhibition of sensory neurite outgrowth and repulsion. (A) Representative images and quantification of DRG neurite outgrowth recovery for CSPGs purified from treated astrocytes relative to CSPGs purified from untreated astrocytes. Data represent the mean \pm S.E.M. from three experiments. $n = 20$ -80 cells per experiment. (B) Representative images and quantification of neurite crossing for DRG neurons grown in the presence of a boundary (shown in red) of CSPGs purified from treated or untreated astrocytes. Data represent the mean \pm S.E.M. from five experiments. $n = 20$ -40 cells per experiment. * $P < 0.05$, ** $P < 0.01$, n.s. = not significant. For A, P values are calculated relative to growth on CSPGs from untreated astrocytes. (Scale bars: 50 μm .)

The ability to inhibit GAG sulfation after CNS injury could have important implications for neural regeneration. After CNS injury, reactive astrocytes enter the site of injury and secrete CSPGs as a means to prevent further damage.⁹⁻¹¹ Previous studies in our laboratory have established that the CS-E sulfation motif is upregulated on these CSPGs and inhibits the growth of sensory axons.¹⁷ Thus, we first examined whether **34** could modulate CS-E expression levels on CSPG-secreting Neu7 astrocytes.⁴⁸ Indeed, astrocytes treated with 10 μM or 25 μM of **34** showed a significant, dose-dependent decrease in cell-surface CS-E expression, as indicated by immunostaining with a CS-E-specific antibody⁴⁹ (Figure 3A and 3B). Notably, no cytotoxicity was observable at the concentrations tested when analyzed by the trypan blue exclusion assay (up to 25 μM). By comparison, sodium chlorate did not reduce CS-E levels to as large an extent, even at doses as high as 25 mM. Similar results were obtained using NIH3T3 fibroblasts, where significant loss of CS-E expression was observed upon treatment with **34**, and **34** had superior potency compared to sodium chlorate (Figure S11).

To characterize the effects of **34** on secreted CSPGs, we purified

the CSPGs from Neu7-conditioned media, digested them with chondroitinase ABC (ChABC), and analyzed their disaccharide composition by reverse-phase ion-pair high-performance liquid chromatography (RPIP-HPLC). CSPGs secreted from Neu7 astrocytes treated with 25 μM of **34** displayed a $62.9 \pm 17.0\%$ increase in unsulfated chondroitin (uCS) content compared to CSPGs secreted from untreated astrocytes, indicating a decrease in overall sulfation (Figure 3C, Table S2). This overall decrease was accompanied by a specific $67.8 \pm 10.9\%$ reduction in the CS-E sulfation motif on secreted CSPGs. Although other CS sulfation motifs were also affected, the CS-E motif was reduced to the largest extent (Figure S12). By comparison, CSPGs secreted from sodiumchlorate-treated cells also displayed lower sulfation compared to untreated cells, albeit to a lesser degree and only in the presence of high concentrations of sodium chlorate ($39.7 \pm 15.6\%$ increase in uCS; $31.6 \pm 10.9\%$ decrease in CS-E).

Having shown that **34** can effectively inhibit CS-E sulfation levels on both surface-expressed and secreted CSPGs, we next examined whether this mode of inhibition could be exploited to stimulate axonal growth. Sensory dorsal root ganglion neurons (DRGs) adjacent to the rat spinal cord were grown on a substratum coated with the CSPGs secreted from Neu7 astrocytes treated with or without **34**. The effects of the CSPGs on neurite outgrowth were determined by immunostaining for the neuronal-specific marker, β III-tubulin, and quantifying the average neurite length. To our delight, we observed a significant, dose-dependent promotion of neurite outgrowth ($30.7 \pm 2.5\%$ at 25 μM of **34**) when DRGs were grown on CSPGs secreted from treated astrocytes compared to untreated astrocytes (Figure 4A). The observed effects could stem from direct inhibition of Chst15 and/or indirect effects on other GAG sulfotransferases such as Chst11, which creates the substrate for Chst15. These results highlight not only the ability of **34** to block known functions of CSPGs but also the potential value of pan-specific GAG sulfotransferase inhibitors. In many cases, the relative contributions of various sulfation motifs and GAG subclasses have not been fully investigated; thus, pan-specific inhibitors may be ideal and enable validation of therapeutic hypotheses.

CNS injury induces tissue damage and leads to formation of a glial scar, which consists predominantly of reactive astrocytes and CSPGs.⁹⁻¹¹ The glial scar serves as a major barrier to axon regeneration. We used an *in vitro* boundary assay to simulate the glial scar and assess the ability of **34** to reverse the inhibitory activity of CSPGs. In this assay, purified CSPGs from Neu7 astrocytes treated with or without **34** were mixed with Texas Red dye and spotted onto glass coverslips. DRG neurons were plated onto the coverslips, and the percentage of neurites that crossed the CSPG boundary was quantified. Whereas DRG neurites were strongly repelled by CSPGs from untreated astrocytes, they crossed more freely into boundaries of CSPGs from astrocytes treated with **34** (Figure 4B). Thus, compound **34** rendered CSPGs more permissive to axonal growth, demonstrating its ability to modulate sulfation-dependent cellular processes.

Finally, we evaluated the potential to use inhibitor **34** *in vivo* by profiling its absorption, distribution, metabolism, and elimination (ADME) properties. **34** showed good stability in human, mouse and rat liver microsomes based on intrinsic clearance (Table S3). The *in vivo* pharmacokinetic (PK) properties of **34** were also evaluated directly in rats. After intravenous injection of compound **34** at a dose of 3.0 mg/kg, the compound had a moderate clearance of

21 mL/min/kg, moderate volume of distribution of 0.97 L/kg, and short terminal half-life of 1.6 h (Table S4). These data suggest that direct application of the compound, as opposed to intravenous injection, may be more efficacious for future use *in vivo*. Taken together, our studies demonstrate that the sulfotransferase inhibitor **34** can diminish the inhibitory effects of CSPGs, and they highlight its promise to be used for the stimulation of neuronal repair.

CONCLUSION

GAG sulfotransferase inhibitors have the potential to be powerful pharmacological tools for elucidating the diverse physiological functions of GAGs and serve as potential therapeutic leads for spinal cord regeneration and human diseases. We report here the discovery of the first cell-permeable, small-molecule inhibitor selective for GAG sulfotransferases. Inhibitor **34** was derived from a high-throughput screen targeted against the CS-E sulfotransferase Chst15 and potently inhibited the sulfation of surface-expressed and secreted CSPGs. Importantly, by decreasing sulfation levels on CSPGs, compound **34** reversed the growth inhibitory effects of CSPGs on sensory axons. These studies demonstrate, for the first time, the ability to modulate a class of enzymes for which, despite high interest, no cell-permeable, small-molecule inhibitors exist. Furthermore, they highlight the promise of using a sulfotransferase inhibitor-based strategy, and potentially **34** or its derivatives, for the stimulation of neuronal growth after injury, stroke, or neurodegenerative disease. Finally, compound **34** provides a lead scaffold that may be further developed to target individual sulfotransferases with high specificity. Owing to the major lack of tools for studying sulfation, we envision that chemically-tuned small molecules capable of modulating specific GAG sulfation patterns will find extensive use as tools in manipulating and understanding GAG-dependent physiological and pathological processes.

METHODS

Detailed experimental procedures are provided in the Supporting Information.

ASSOCIATED CONTENT

Supporting Information

The Supporting Information is available free of charge on the ACS Publications website at DOI:

Experimental methods, compound characterizations, supporting figures, and tables (PDF)

AUTHOR INFORMATION

Corresponding Author

lhw@caltech.edu

Notes

The authors declare no competing financial interests.

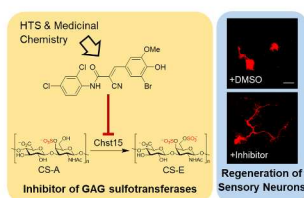
ACKNOWLEDGMENT

We would like to thank the Beckman Institute Laser Resource Center at Caltech for use of the Fluorolog 3 instrument, A. Fisher for providing APS kinase, L. Pedersen for providing Hs3st1 and Sult2b1a/b vectors, and H. Geller for providing the Neu7 astrocyte cell line. This work was supported by grants from the NIH (R01 GM093627 (L.C.H.-W.) and NIH/NRSA 5T32 GM07616 (S.T.C.)).

REFERENCES

- (1) Capila, I., and Linhardt, R. J. (2002) Heparin-protein interactions. *Angew. Chem. Int. Edit.* *41*, 391-412.
- (2) Shukla, D., Liu, J., Blaiklock, P., Shworak, N. W., Bai, X., Esko, J. D., Cohen, G. H., Eisenberg, R. J., Rosenberg, R. D., and Spear, P. G. (1999) A novel role for 3-O-sulfated heparan sulfate in herpes simplex virus 1 entry. *Cell* *99*, 13-22.
- (3) Xu, D., and Esko, J. D. (2014) Demystifying heparan sulfate-protein interactions. *Annu. Rev. Biochem.* *83*, 129-157.
- (4) Kim, S. Y., Zhao, J., Liu, X., Fraser, K., Lin, L., Zhang, X., Zhang, F., Dordick, J. S., and Linhardt, R. J. (2017) Interaction of Zika virus envelope protein with glycosaminoglycans. *Biochemistry* *56*, 1151-1162.
- (5) Fuster, M. M., and Esko, J. D. (2005) The sweet and sour of cancer: glycans as novel therapeutic targets. *Nat. Rev. Cancer* *5*, 526-542.
- (6) Sasisekharan, R., Shriver, Z., Venkataraman, G., and Narayanasami, U. (2002) Roles of heparan-sulphate glycosaminoglycans in cancer. *Nat. Rev. Cancer* *2*, 521-528.
- (7) Mizumoto, S., Yamada, S., and Sugahara, K. (2015) Molecular interactions between chondroitin-dermatan sulfate and growth factors/receptors/matrix proteins. *Curr. Opin. Struct. Biol.* *34*, 35-42.
- (8) Hacker, U., Nybakken, K., and Perrimon, N. (2005) Heparan sulphate proteoglycans: the sweet side of development. *Nat. Rev. Mol. Cell Biol.* *6*, 530-541.
- (9) Carulli, D., Laabs, T., Geller, H. M., and Fawcett, J. W. (2005) Chondroitin sulfate proteoglycans in neural development and regeneration. *Curr. Opin. Neurobiol.* *15*, 116-120.
- (10) Yiu, G., and He, Z. (2006) Glial inhibition of CNS axon regeneration. *Nat. Rev. Neurosci.* *7*, 617-627.
- (11) Busch, S. A., and Silver, J. (2007) The role of extracellular matrix in CNS regeneration. *Curr. Opin. Neurobiol.* *17*, 120-127.
- (12) Miller, G. M., and Hsieh-Wilson, L. C. (2015) Sugar-dependent modulation of neuronal development, regeneration, and plasticity by chondroitin sulfate proteoglycans. *Exp. Neurol.* *274*, 115-125.
- (13) Raman, R., Sasisekharan, V., and Sasisekharan, R. (2005) Structural insights into biological roles of protein-glycosaminoglycan interactions. *Chem. Biol.* *12*, 267-277.
- (14) Rogers, C. J., Clark, P. M., Tully, S. E., Abrol, R., Garcia, K. C., Goddard, W. A., and Hsieh-Wilson, L. C. (2011) Elucidating glycosaminoglycan-protein-protein interactions using carbohydrate microarray and computational approaches. *Proc. Natl. Acad. Sci. U.S.A.* *108*, 9747-9752.
- (15) Gama, C. I., and Hsieh-Wilson, L. C. (2005) Chemical approaches to deciphering the glycosaminoglycan code. *Curr. Opin. Chem. Biol.* *9*, 609-619.
- (16) Gama, C. I., Tully, S. E., Sotogaku, N., Clark, P. M., Rawat, M., Vaidehi, N., Goddard, W. A., 3rd, Nishi, A., and Hsieh-Wilson, L. C. (2006) Sulfation patterns of glycosaminoglycans encode molecular recognition and activity. *Nat. Chem. Biol.* *2*, 467-473.
- (17) Brown, J. M., Xia, J., Zhuang, B., Cho, K. S., Rogers, C. J., Gama, C. I., Rawat, M., Tully, S. E., Uetani, N., Mason, D. E., Tremblay, M. L., Peters, E. C., Habuchi, O., Chen, D. F., and Hsieh-Wilson, L. C. (2012) A sulfated carbohydrate epitope inhibits axon regeneration after injury. *Proc. Natl. Acad. Sci. U. S. A.* *109*, 4768-4773.
- (18) Chapman, E., Best, M. D., Hanson, S. R., and Wong, C. H. (2004) Sulfotransferases: structure, mechanism, biological activity, inhibition, and synthetic utility. *Angew. Chem. Int. Edit.* *43*, 3526-3548.
- (19) Kusche-Gullberg, M., and Kjellen, L. (2003) Sulfotransferases in glycosaminoglycan biosynthesis. *Curr. Opin. Struct. Biol.* *13*, 605-611.
- (20) Habuchi, O. (2000) Diversity and functions of glycosaminoglycan sulfotransferases. *Bba-Gen. Subjects* *1474*, 115-127.

- (21) Negishi, M., Pedersen, L. G., Petrotchenko, E., Shevtsov, S., Gorokhov, A., Kakuta, Y., and Pedersen, L. C. (2001) Structure and function of sulfotransferases. *Arch. Biochem. Biophys.* **390**, 149-157.
- (22) Brown, J. R., Nishimura, Y., and Esko, J. D. (2006) Synthesis and biological evaluation of gem-diamine 1-N-iminosugars related to L-iduronic acid as inhibitors of heparan sulfate 2-O-sulfotransferase. *Bioorg. Med. Chem. Lett.* **16**, 532-536.
- (23) Nozaki, H., Tomoyama, Y., Takagi, H., Yokoyama, K., Yamada, C., Kaio, K., Tsukimori, M., Nagao, K., Itakura, Y., Ohtake-Niimi, S., Nakano, H., and Habuchi, O. (2010) Inhibition of N-acetylgalactosamine 4-sulfate 6-O-sulfotransferase by beta-D-4-O-sulfo-N-acetylgalactosaminides bearing various hydrophobic aglycons. *Glycoconjugate J.* **27**, 237-248.
- (24) Gesteira, T. F., Coulson-Thomas, V. J., Taunay-Rodrigues, A., Oliveira, V., Thacker, B. E., Juliano, M. A., Pasqualini, R., Arap, W., Tersariol, I. L., Nader, H. B., Esko, J. D., and Pinhal, M. A. (2011) Inhibitory peptides of the sulfotransferase domain of the heparan sulfate enzyme, N-deacetylase-N-sulfotransferase-1. *J. Biol. Chem.* **286**, 5338-5346.
- (25) Rath, V. L., Verdugo, D., and Hemmerich, S. (2004) Sulfotransferase structural biology and inhibitor discovery. *Drug Discov. Today* **9**, 1003-1011.
- (26) Hemmerich, S., Verdugo, D., and Rath, V. L. (2004) Strategies for drug discovery by targeting sulfation pathways. *Drug Discov. Today* **9**, 967-975.
- (27) Li, F., ten Dam, G. B., Murugan, S., Yamada, S., Hashiguchi, T., Mizumoto, S., Oguri, K., Okayama, M., van Kuppevelt, T. H., and Sugahara, K. (2008) Involvement of highly sulfated chondroitin sulfate in the metastasis of the Lewis lung carcinoma cells. *J. Biol. Chem.* **283**, 34294-34304.
- (28) Cole, C. L., Rushton, G., Jayson, G. C., and Avizienyte, E. (2014) Ovarian cancer cell heparan sulfate 6-O-sulfotransferases regulate an angiogenic program induced by heparin-binding epidermal growth factor (EGF)-like growth factor/EGF receptor signaling. *J. Biol. Chem.* **289**, 10488-10501.
- (29) Sepulveda-Diaz, J. E., Naini, S. M. A., Huynh, M. B., Ouidja, M. O., Yanicostas, C., Chantepie, S., Villares, J., Lamari, F., Jospin, E., van Kuppevelt, T. H., Mensah-Nyagan, A. G., Raisman-Vozari, R., Soussi-Yanicostas, N., and Papy-Garcia, D. (2015) HS3ST2 expression is critical for the abnormal phosphorylation of tau in Alzheimer's disease-related tau pathology. *Brain* **138**, 1339-1354.
- (30) Plaas, A. H., West, L. A., Wong-Palms, S., and Nelson, F. R. (1998) Glycosaminoglycan sulfation in human osteoarthritis. Disease-related alterations at the non-reducing termini of chondroitin and dermatan sulfate. *J. Biol. Chem.* **273**, 12642-12649.
- (31) Kluppel, M., Wight, T. N., Chan, C., Hinek, A., and Wrana, J. L. (2005) Maintenance of chondroitin sulfation balance by chondroitin-4-sulfotransferase 1 is required for chondrocyte development and growth factor signaling during cartilage morphogenesis. *Development* **132**, 3989-4003.
- (32) Fried, M., and Duffy, P. E. (1996) Adherence of Plasmodium falciparum to chondroitin sulfate A in the human placenta. *Science* **272**, 1502-1504.
- (33) Achur, R. N., Kakizaki, I., Goel, S., Kojima, K., Madhunapantula, S. V., Goyal, A., Ohta, M., Kumar, S., Takagaki, K., and Gowda, D. C. (2008) Structural interactions in chondroitin 4-sulfate mediated adherence of Plasmodium falciparum infected erythrocytes in human placenta during pregnancy-associated malaria. *Biochemistry* **47**, 12635-12643.
- (34) Akama, T. O., Nishida, K., Nakayama, J., Watanabe, H., Ozaki, K., Nakamura, T., Dota, A., Kawasaki, S., Inoue, Y., Maeda, N., Yamamoto, S., Fujiwara, T., Thonar, E. J., Shimomura, Y., Kinoshita, S., Tanigami, A., and Fukuda, M. N. (2000) Macular corneal dystrophy type I and type II are caused by distinct mutations in a new sulphotransferase gene. *Nat. Genet.* **26**, 237-241.
- (35) Greve, H., Cully, Z., Blumberg, P., and Kresse, H. (1988) Influence of chlorate on proteoglycan biosynthesis by cultured human fibroblasts. *J. Biol. Chem.* **263**, 12886-12892.
- (36) Smith-Thomas, L. C., Stevens, J., Fok-Seang, J., Faissner, A., Rogers, J. H., and Fawcett, J. W. (1995) Increased axon regeneration in astrocytes grown in the presence of proteoglycan synthesis inhibitors. *J. Cell Sci.* **108**, 1307-1315.
- (37) Ullrich, T. C., and Huber, R. (2001) The complex structures of ATP sulfurylase with thiosulfate, ADP and chlorate reveal new insights in inhibitory effects and the catalytic cycle. *J. Mol. Biol.* **313**, 1117-1125.
- (38) Baeuerle, P. A., and Huttner, W. B. (1986) Chlorate - a potent inhibitor of protein sulfation in intact-cells. *Biochem. Biophys. Res. Commun.* **141**, 870-877.
- (39) Steffen, C., and Wetzel, E. (1993) Chlorate poisoning: mechanism of toxicity. *Toxicology* **84**, 217-231.
- (40) Ohtake, S., Ito, Y., Fukuta, M., and Habuchi, O. (2001) Human N-acetylgalactosamine 4-sulfate 6-O-sulfotransferase cDNA is related to human B cell recombination activating gene-associated gene. *J. Biol. Chem.* **276**, 43894-43900.
- (41) Chapman, E., Ding, S., Schultz, P. G., and Wong, C. H. (2002) A potent and highly selective sulfotransferase inhibitor. *J. Am. Chem. Soc.* **124**, 14524-14525.
- (42) Burkart, M. D., Izumi, M., Chapman, E., Lin, C. H., and Wong, C. H. (2000) Regeneration of PAPS for the enzymatic synthesis of sulfated oligosaccharides. *J. Org. Chem.* **65**, 5565-5574.
- (43) Serafimova, I. M., Pufall, M. A., Krishnan, S., Duda, K., Cohen, M. S., Maglathlin, R. L., McFarland, J. M., Miller, R. M., Frodin, M., and Taunton, J. (2012) Reversible targeting of noncatalytic cysteines with chemically tuned electrophiles. *Nat. Chem. Biol.* **8**, 471-476.
- (44) Krishnan, S., Miller, R. M., Tian, B., Mullins, R. D., Jacobson, M. P., and Taunton, J. (2014) Design of reversible, cysteine-targeted Michael acceptors guided by kinetic and computational analysis. *J. Am. Chem. Soc.* **136**, 12624-12630.
- (45) Weerapana, E., Wang, C., Simon, G. M., Richter, F., Khare, S., Dillon, M. B. D., Bachovchin, D. A., Mowen, K., Baker, D., and Cravatt, B. F. (2010) Quantitative reactivity profiling predicts functional cysteines in proteomes. *Nature* **468**, 790-795.
- (46) Kobayashi, M., Sugumaran, G., Liu, J. A., Shworak, N. W., Silbert, J. E., and Rosenberg, R. D. (1999) Molecular cloning and characterization of a human uronyl 2-sulfotransferase that sulfates iduronyl and glucuronyl residues in dermatan chondroitin sulfate. *J. Biol. Chem.* **274**, 10474-10480.
- (47) Aikawa, J., Grobe, K., Tsujimoto, M., and Esko, J. D. (2001) Multiple isozymes of heparan sulfate/heparin GlcNAc N-deacetylase/GlcN N-sulfotransferase - structure and activity of the fourth member, NDST4. *J. Biol. Chem.* **276**, 5876-5882.
- (48) Fok-Seang, J., Smith-Thomas, L. C., Meiners, S., Muir, E., Du, J. S., Housden, E., Johnson, A. R., Faissner, A., Geller, H. M., Keynes, R. J., Rogers, J. H., and Fawcett, J. W. (1995) An analysis of astrocytic cell lines with different abilities to promote axon growth. *Brain Res.* **689**, 207-223.
- (49) Tully, S. E., Rawat, M., and Hsieh-Wilson, L. C. (2006) Discovery of a TNF-alpha antagonist using chondroitin sulfate microarrays. *J. Am. Chem. Soc.* **128**, 7740-7741.

1
2
3
4
5
6
7
8
9
10
11
12
13
14
15
16
17
18
19
20
21
22
23
24
25
26
27
28
29
30
31
32
33
34
35
36
37
38
39
40
41
42
43
44
45
46
47
48
49
50
51
52
53
54
55
56
57
58
59
60

215x279mm (300 x 300 DPI)